Sensors and Materials, Vol. 35, No. 9 (2023) 3137–3149
MYU Tokyo

S & M 3380

Development of Wearable-assist-clothing Control Based on Electrical Activities in Lower-limb Muscles

Atsushi Tsukahara,[1*] Shuta Yamamoto,[2] and Sho Hirota[3]

[1]Assistive Robot Center, National Center for Geriatrics and Gerontology,
7-430 Morioka, Obu, Aichi 474-8511, Japan
[2]Department of Biomedical Engineering, Graduate School of Science and Technology, Shinshu University,
3-15-1 Tokida, Ueda, Nagano 386-8567, Japan
[3]Mechanical Design Section, Technology Center, R&D Unit, VAIO Corporation,
5432 Toyoshina, Azumino, Nagano 399-8282, Japan

(Received May 9, 2023; accepted August 9, 2023)

Keywords: inflatable actuator, soft exosuit, voluntary control, EMG, assistive robot, wearable robotics

The aim of this study is to develop a novel soft exosuit called inflatable assist clothing (InAC) with lightweight and flexible inflatable actuators (IfAs) and to propose a voluntary control method to control the IfA using electrical changes during muscle activity. The InAC is equipped with IfAs, which generate a contraction force by supplying compressed air from a DC vacuum pump with compressor function to assist with knee flexion and extension. In addition, our proposed control method, the bioelectrical signal (BES)-based control algorithm, estimates the desired air volume to be supplied by the DC pump to each individual IfA on the basis of the displacement volume of the BES and then performs feedback control to track the desired air volume. In this study, the control verification experiments were conducted to investigate whether the compressed air volume discharged toward the IfA was changed by using the BES measured from the rectus femoris muscle. The results indicated that the proposed algorithm embedded in the InAC can control the internal air volume of the IfA on the basis of the BES displacement while also tracking the desired air volume (mean absolute error: 3.03 mL; mean absolute percentage error: 6.85%).

1. Introduction

The percentage of the population aged 65 and over has continued to increase worldwide. In particular, the shares of the population aged 65 and over in Eastern and Southeastern Asia, Australia and New Zealand, and Europe and Northern America are projected to increase rapidly to 25.7, 23.7, and 26.9%, respectively, by 2050.(1) The musculoskeletal diseases associated with such a super-aged society deteriorate the ability of elderly people to walk independently, which can increase the risk of requiring long-term care or support. Furthermore, Terai *et al.* reported that the rate of incidence of a locomotive syndrome, which is a condition of an increased risk of requiring long-term care because of a lack of exercise or age-associated decline causing muscle

*Corresponding author: e-mail: tsukahara@ncgg.go.jp
https://doi.org/10.18494/SAM4502

ISSN 0914-4935
https://myukk.org/

weakness, has increased considerably as a result of the COVID-19 pandemic.[2,3] Gait disturbance due to population aging and the locomotive syndrome is a common social issue worldwide that must be resolved to promote independent living and increase the healthy life expectancy of the population.

Wearable assistive robots, which support the wearer's legged locomotion, provide an effective solution to aid the recovery of the motor and sensory functions in the lower limbs efficiently and to address the social issue mentioned above. To date, gait training using wearable assistive robots has mainly been performed for patients that have suffered a stroke, a spinal cord injury, or an intractable neurological disease,[4–6] whereas more recent studies have been focused on the provision of walking support for elderly people and patients with locomotive syndrome.[7–10] Exoskeletal robots for the elderly and locomotive syndrome patients assist their hip flexion and extension by providing assistive torque generated from DC motors attached to the hip joint parts via rigid exoskeletal frames. Therefore, the total weights of these systems are lower than those of previously developed exoskeleton robots. However, physical misalignment of the rotational axis between the exoskeletal robot and the wearer's lower limb may generate unnecessary disturbance forces that adversely affect the assistive performance, and excessive clamping pressure from the cuffs that fix the exoskeletal frame to the lower limbs may cause discomfort to the wearer.[11]

To avoid these structural issues of rigid exoskeletal robots, soft exosuits have recently been developed for use in the wearable assistive robotics field. The soft exosuits are broadly classified into pneumatic artificial muscles (PAMs) type and a motor-driven tendon tensile type, depending on the applied actuator. The exosuits using PAMs of McKibben type or pneumatic gel muscles (PGMs) consist of flexible, tubular sleeves made of rubber or styrene-based thermoplastic elastomer as actuators, respectively.[12–15] Since these actuators generate a contraction force along the length of the wearer's muscle fibers while expanding radially in the tubular sleeves by supplying compressed air, the exosuits using the PAMs can provide the gait assistance without traditional rigid exoskeletal structures. However, considering the application in daily life, the hardware design, in which the PAMs are attached over the wearer's clothing and the change in the shape of the PAMs, including expansion and contraction, is used to assist the wearer's movement, still has critical issues of affinity with the clothing and stigma of physical illness.[16] Meanwhile, the soft exosuits using motor-driven tendon tensile type have been developed to address the issues of soft exosuits with PAMs. Wyss Institute at Harvard University has developed a soft exosuit that generates tensile force in Bowden cables attached to the exosuit by driving a geared motor, thus assisting multiple joints of the wearer during walking (e.g., ankle plantarflexion with hip flexion and extension,[17] knee extension,[18] and hip abduction[19]). The ReWalk ReStore™ exosuit, developed by ReWalk Robotics Ltd., also transmits torque generated by an actuator to the exosuit via Bowden cables to assist the wearer with ankle dorsiflexion and plantarflexion.[20,21] Moreover, a group from Arizona State University has developed a soft-inflatable exosuit to help with knee extension using inflatable soft actuators designed from heat-sealable thermoplastic polyurethane (TPU) films with a circular cross section and encased in fabric so as to further enhance affinity with clothing.[22–24] That system demonstrated the decreasing BES of healthy subjects in the quadriceps by assisting knee extension in the swing and initial stance phase during walking on a treadmill.

Most of these soft exosuits detect the moment at which the swing phase begins in the gait cycle using a gyroscope sensor, inertial measurement units (IMUs), a strain gauge, or ground reaction force sensors, and then supply an assistive force with the desired trajectory to the wearer's leg during the swing phase. However, when the applications of these devices in daily life are considered, the soft exosuits are required to perform various motion assistance tasks in the lower limbs as well as walking assistance. Therefore, it is still challenging to realize further versatile motion assistance actions based on the wearer's voluntary motion intention for the current soft exosuits, which must detect only gait events and provide prepared target trajectories in advance.

In contrast, the assistive method of traditional wearable robots with rigid exoskeletal frames, which is based on the detection of bioelectrical signals (BESs) from the skin surface immediately before the corresponding muscle contraction, is used widely as a valuable means to reflect the wearer's intended motion to the various forms of motion assistance.[4,9,25–27] From the examples described above, to allow more versatile motion assistance actions to be realized when using a soft exosuit with lightweight and flexible structures, it is vital to establish a seamless interactive motion control method that acts between the robot and the wearer in accordance with the muscle activities in the wearer's body.

The purpose of this study is thus to develop soft inflatable assist clothing called InAC with a lightweight and flexible inflatable actuator (IfA) and to propose a voluntary control method to control the IfA on the basis of the displacement volume of the BES. To this end, we evaluated the usefulness of the developed and proposed system through an IfA control verification experiment using the BES of the lower limb during knee flexion and extension.

2. System Design

2.1 Inflatable assist clothing (InAC)

We developed the soft exosuit InAC,[28] as shown in Fig. 1, to support knee flexion and extension for elderly and locomotive syndrome patients in the maintenance phase who require regular walking support to prevent unexpected stumbling or falls in daily life after undergoing exercise training at a rehabilitation center. The InAC mainly consists of contraction-type IfAs, BES sensors, internal pressure sensors, IMUs, and a control unit. The IfA is composed of multiple inflatable chambers, as illustrated in Fig. 2(a), and is fabricated by heat sealing two thin TPU layers. The compressed air from a brushless-DC-motor-driven diaphragm vacuum pump with compressor function (DP0210TA-Y1, NITTO KOHKI Co., Ltd., Japan) flows into the multiple inflatable chambers via the unsealed narrow longitudinal air slits in the middle of the IfA. The expansion of the inflatable chambers in the thickness direction through pneumatic filling generates an overall longitudinal contraction of the IfA, as shown in Fig. 2(b). The proximal end of the IfA is attached to an inelastic fabric sewn onto elastic leggings using snap buttons, and the distal end of the IfA is connected via nylon wires to a restraining strap attached to the lower part of the patella. The IfAs are positioned at the front and back surfaces of both thighs in the wearing arrangement described above. Switching between air supply and exhaust

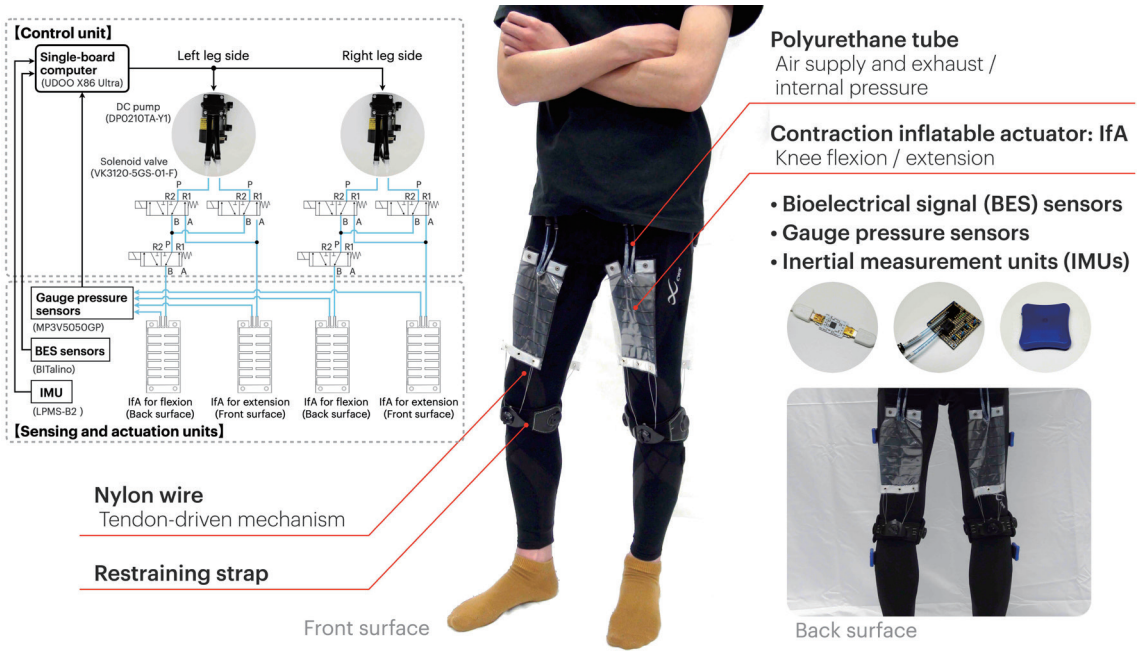

Fig. 1. (Color online) System configurations of inflatable assist clothing (InAC).

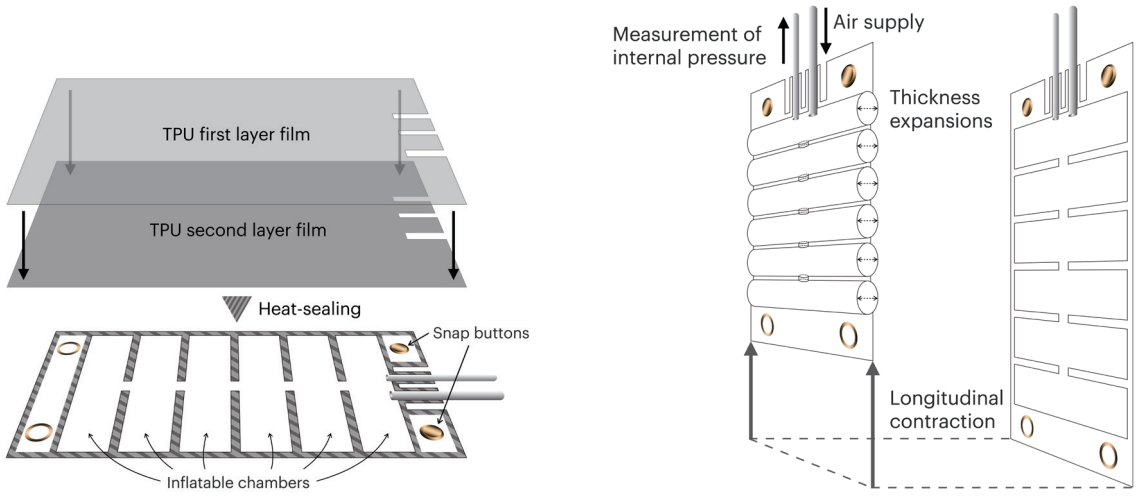

(a) (b)

Fig. 2. (Color online) (a) Schematic of IfA with TPU films, where diagonal stripe lines indicate heat-sealed area. (b) Illustration of the longitudinal contraction on supplying compressed air.

of the relevant IfAs is performed using solenoid valves (VK3120-5GS-01-F, SMC Corporation, Japan), and the contraction forces generated by the IfAs then assist the wearer with knee flexion and extension.

The BES sensors (BITalino, PLUX Wireless Biosignals S.A., Portugal) are used to control the IfAs voluntarily, using the electrical changes in muscle activity detected from the skin surface immediately before the muscle contraction occurs (this will be described in Sect. 2.2). The internal pressure of each IfA is measured using IfA-connected gauge pressure sensors (MP3V5050GP, NXP USA, Inc., USA). The wireless IMUs (LPMS-B2, LP-Research Inc., Japan) are placed on the sacral region and on the thighs and lower thighs to process the measured leg motions with the InAC controller and then calculate the hip and knee joint angles in real time.

The InAC control unit contains a single-board computer (UDOO X86 Ultra, SECO S.p.A, Italy), two DC vacuum pumps with compressor function, and six solenoid valves. The total weight of the control unit is about 1.42 kg. The single-board computer is equipped with a quad-core Intel® Pentium® N3710 processor (Intel® Braswell) and an Arduino™ 101-compatible platform (Intel® Curie) on the same board. In addition, it can provide seamless intercommunication between the processor and the platform. Although the InAC system can be worn by the user on their body, all units other than the sensing units (i.e., the IMUs and BES sensors) used in this study were situated off-board to investigate the usefulness of voluntary control of the IfA using the changes in the BES.

2.2 BES-based contraction control of inflatable actuators

In this paper, we propose a BES-based control algorithm to enable voluntary adjustment of the air volume supplied by the DC vacuum pump to the IfA in accordance with the BES displacement. Figure 3 shows the proposed InAC system control scheme, which consists of an IfA contraction force translator, a contraction force–air volume profile (*C–A* profile), an internal pressure air volume profile (*I–A* profile), and a feedback controller. The details and the relationships between these components are described in the following sub-subsections.

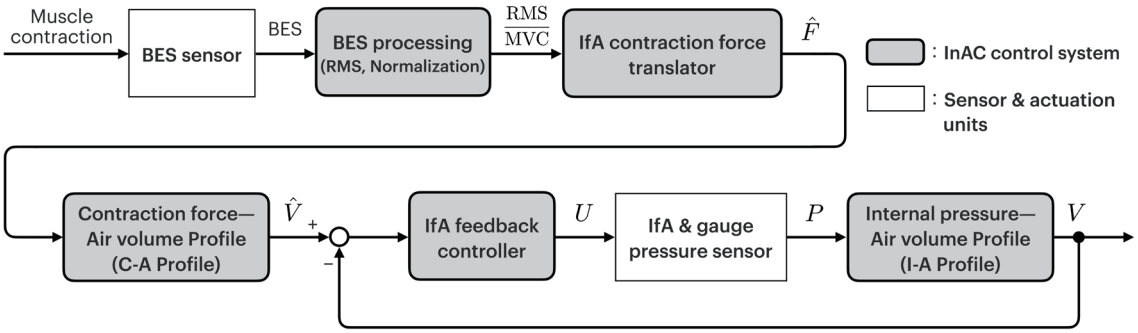

Fig. 3. Control scheme of the InAC system. First, the normalized BES is converted into $\hat{F}$ via the IfA contraction force translator. Next, the desired air volume $\hat{V}$ of the IfA, which corresponds to $\hat{F}$, is calculated using the *C–A* profile. Simultaneously, the internal air volume V of the IfA, which corresponds to the internal pressure P of the IfA measured by the gauge pressure sensor, is calculated using the *I–A* profile. Finally, the InAC system conducts closed-loop control utilizing the feedback from V to attain $\hat{V}$ estimated on the basis of the normalized BES.

2.2.1 IfA contraction force calculator

The muscle contraction as a voluntary muscle activity is measured from the BES, including the muscle potential detected from the skin surface. The measured BES is rectified by calculating its root mean square (*RMS*) value using a moving average window of 40 ms. The RMS value of the BES is normalized using isometric maximal voluntary contraction (*MVC*). The IfA contraction force translator then converts this normalized BES into the desired IfA contraction force $\hat{F}$, as follows:

$$\hat{F} = \frac{RMS}{MVC} \cdot F_{max}, \tag{1}$$

where F_{max} is the maximum contraction force of the IfA when the compressed air from the DC vacuum pump fills the IfA completely.

2.2.2 Contraction force–air volume profile (*C–A* profile)

The air volume required for longitudinal contraction of the IfA must be estimated using $\hat{F}$ of Eq. (1), because the IfA's built-in gauge pressure sensor measures the internal pressure while the IfA is being driven. Therefore, we conducted preliminary experiments on isometric contraction of the IfA, in which the IfA contraction force is measured while the length of the IfA in the longitudinal direction remains constant during the air supply phase, to derive the relationship between the air volume and the contraction force. From the results of these experiments, we designed the *C–A* profile as shown in Fig. 4(a) to estimate the desired air volume $\hat{V}$ to be supplied to the IfA for the corresponding $\hat{F}$. The $\hat{V}$ value is calculated using the *C–A* profile as follows:

$$\hat{V} = -1.3 \cdot 10^{-3} F^4 + 9.4 \cdot 10^{-2} F^3 - 2.0 \cdot F^2 + 18.0 \cdot F + 8.5. \tag{2}$$

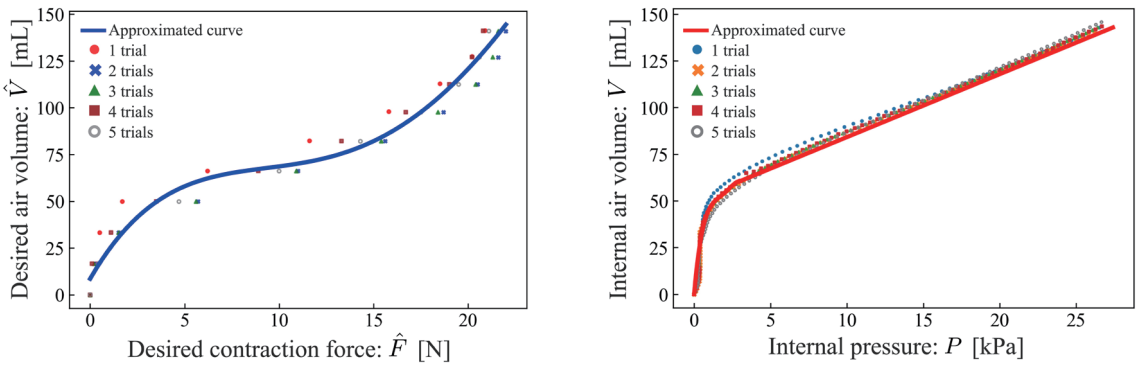

(a) (b)

Fig. 4. (Color online) Constructed profiles based on preliminary results of IfA isometric contraction: (a) *C–A* profile for $\hat{V}$ vis-a-vis $\hat{F}$ and (b) *I–A* profile for *V* vis-a-vis *P*. Blue and red lines denote the approximated curves of the *C–A* profile and the *I–A* profile, respectively.

2.2.3 Internal pressure–air volume profile (*I–A* profile)

It is essential to infer the internal air volume of the IfA to enable feedback control to be performed using the $\hat{V}$ calculated as the desired value from the *C–A* profile. In this study, the relationship between the internal air volume and the internal pressure was also derived by performing IfA isometric contraction experiments, similar to the case of the relationship between the contraction force $\hat{F}$ and the air volume $\hat{V}$. The *I–A* profile, from which the internal air volume V corresponding to the internal pressure P of the IfA is obtained, was designed using the results of these experiments, as shown in Fig. 4(b). The V with respect to the *I–A* profile is calculated as follows:

$$V = \begin{cases} -2.8P^4 + 0.23\cdot10^{-2}P^3 - 0.67\cdot10^{-2}P^2 + 0.93\cdot10^{-2}P + 8.2\cdot10^{-2}, & (0 \le P < 3.0) \\ 3.4P + 0.5\cdot10^{-2}, & (3.0 \le P \le P_{max}) \end{cases} \quad (3)$$

where P_{max} is the maximum internal pressure of the IfA when filled completely with the compressed air from the DC vacuum pump.

2.2.4 IfA feedback controller

The InAC system is a closed-loop controller that uses the feedback from the V of the IfA obtained via the *I–A* profile to realize the $\hat{V}$ calculated using the *C–A* profile. The command voltage is controlled via pulse width modulation (PWM) to adjust the amount of compressed air to be supplied in accordance with the change in the BES. The control law with respect to the IfA feedback controller is calculated as follows:

$$U(t) = K_P \cdot e(t), \quad (4)$$

where $U(t)$ is the command voltage as a function of time t; K_P is the proportional gain; and $e(t) = \hat{V} - V$ is the error between the desired and obtained air volumes as a function of t.

3. Experiments

Figure 5 shows the experimental setup used for the verification experiment. In this experiment, the InAC with the proposed BES-based control algorithm was used to conduct knee flexion and extension experiments on a healthy subject in a seated posture. The sensing unit (i.e., the IMU and the BES sensor) was attached to the subject's body. The electrodes used to perform the BES measurements were placed on the rectus femoris muscle (RFM) of the right thigh to control the contraction of the IfA on the basis of the BES displacement volume during the extension of the right knee joint. In addition, a reference electrode was placed on the head of the fibula (see Fig. 5, top right). The proportional gain in Eq. (4) was set at $K_P = 1.2$ to allow the appropriate control to be performed without overshooting and undershooting throughout the results of prior fundamental experiments.

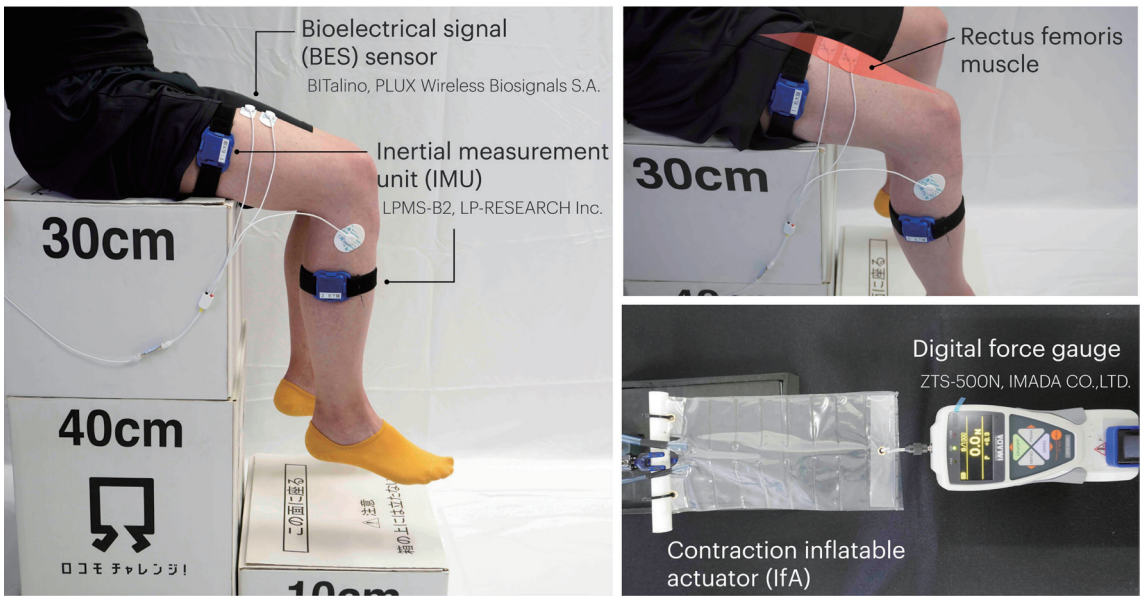

Fig. 5. (Color online) Experimental setup for the verification experiment in this study.

The IfA contraction force was measured using a digital force gauge (ZTS-500N, IMADA Co., Ltd., Japan) without attaching the IfA to the subject's thigh (see Fig. 5, bottom right). Specifically, the proximal end of the IfA was anchored securely to a restraining stand located on an off-board table using zip ties. The distal end of the IfA was connected to a force gauge, which was fixed to the table using a clamp, to measure the isometric contraction force of the IfA generated while maintaining the IfA's longitudinal length when the supply of compressed air created tension.

Table 1 and Fig. 6 show the design parameters and their values for the IfA used in this study. F_{max} and P_{max} are the averaged values of the results obtained from IfA performance evaluation experiments conducted in advance. Specifically, we redefined the averaged contraction force at 80% MVC as F_{max} from a safety standpoint.

In this experiment, the mean absolute error (*MAE*) and the mean absolute percentage error (*MAPE*) were used to investigate the margins of error between V and $\hat{V}$ when the proposed algorithm was applied to knee flexion and extension of the test subject. These analyses were performed using R software (Foundation for Statistical Computing, Vienna, Austria). This study was performed with the approval of the Nagano Prefecture General Industrial Technology Center (Matsumoto, Nagano, Japan) review board.

4. Results and Discussion

Figure 7 shows the results of the subject's knee joint angle, %MVC and BES in the RFM, the internal air volume V and desired air volume $\hat{V}$ of the IfA, and the isometric contraction force of the IfA during the verification experiment when using the InAC system, including the proposed BES-based control algorithm. The subject intentionally adjusted the contraction of the RFM

Table 1
IfA design parameters and their values.

Design parameters	Values
Length (longitudinal direction): L (mm)	159.0
Width (transverse direction): W (mm)	103.0
Number of inflatable chambers: m	7
Length per inflatable chamber: l	21.0
Maximum contraction force (80%MVC): F_{max} (N)	16.6
Maximum internal pressure: P_{max} (kPa)	36.5

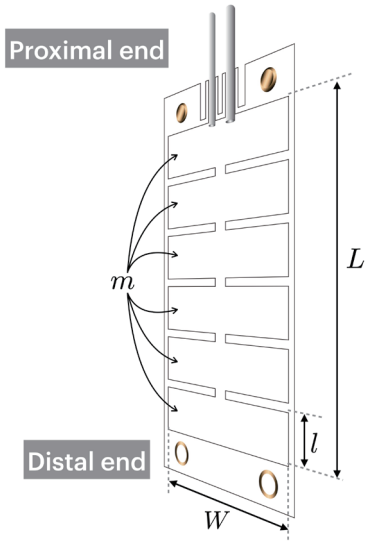

Fig. 6. (Color online) Definition of IfA design parameters shown in Table 1.

during the knee extension movements to investigate whether the compressed air volume supplied to the IfA changes in accordance with changes in the BES.

The results of the obtained and desired air volumes of the IfA given in these figures showed that the internal air volume V calculated using Eq. (3) generally corresponded to the desired air volume $\hat{V}$, which was calculated using Eq. (2) by the feedback control method. The results of *MAE* and *MAPE* between V and $\hat{V}$ were 3.03 mL and 6.85%, respectively. The most significant aspect of these results is that the InAC system controlled the compressed air volume supplied by the DC vacuum pump to the IfA on the basis of the displacement volume of the normalized BES, as indicated by the light gray area in Fig. 7. The IfA contraction force, which was measured using the force gauge, also behaved in a manner dependent on the amount of change in the compressed air.

The goal of the present study was to develop a soft exosuit, i.e., the InAC with the IfA, and to propose the voluntary control method required to control the IfA based on the BES displacement volume. The contribution of this paper is that the InAC system voluntarily controls the compressed air volume supplied to the IfA according to the displacement volume of the BES that reflects the wearer's motion intention, whereas most previous soft exosuits detect the moment of

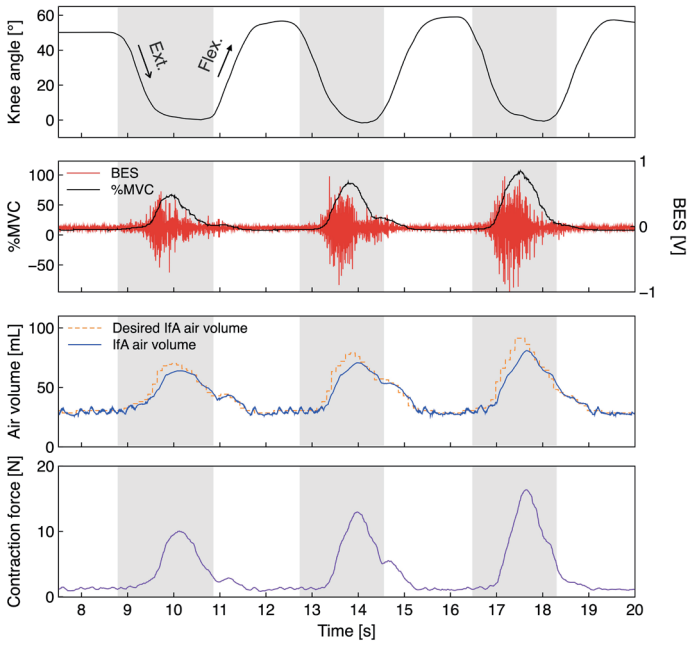

Fig. 7. (Color online) Results of the IfA contraction verification experiments. The %MVC shown as the black line denotes the value of the normalized BES when expressed as a percentage. The desired IfA air volume shown as the dashed orange line was calculated on the basis of the amount of change in the normalized BES using Eq (2). The IfA air volume obtained using Eq. (3), as shown by the blue line, was controlled to correspond to the desired air volume using the IfA feedback controller in accordance with Eq. (4).

the beginning of the moving leg using the sensor readings, i.e., a gyroscope sensor, an IMU, a strain gauge, or ground reaction force sensors and then supply assistive force by the constant motor rotation or the preprogrammed target trajectory.[17–24] The target subjects, therefore, require the physical ability that intentionally produces the movement of the legs to convey the detection of BESs while the muscle contracts the InAC system. In addition, most elderly and locomotive syndrome patients perform daily activities with the anxiety of legged locomotion after discharge from a hospital or a rehabilitation center, even though their symptoms of functional impairment stabilize. From the standpoint of the target subjects who do not require continuous and large assistive force, the soft exosuit InAC that can be integrated with clothes has advantages in adaptability to the wearer's leg motion and wearability compared with a traditional exoskeleton robot. Therefore, the result of our study has clinical importance as the motion support in daily living for elderly people and patients with locomotive syndrome in the maintenance phase.

The effects of the gait support provided by the InAC with the BES-based control algorithm are still unclear at this stage because the limitations of this study include the control of the compressed air volume used for IfA contraction being conducted using a simple feedback controller with proportional control alone and the desired air volume and internal air volume of the IfA being estimated on the basis of the experimental results with low versatility, and the experiment being performed simply to provide operational verification of the control algorithm.

However, it has been reported that a soft inflatable exosuit with a balloon-type inflatable actuator, which exhibits a generated force performance equivalent to that of the exosuit used in this study, potentially assists the wearer's knee extension.[22–24] Hence, it is reasonable to expect that the InAC with the BES-based control method will help the wearer's knee flexion and extension motions efficiently during walking by providing an assistive gain.

We are currently developing an optimization model of the IfAs with high versatility and a feedback control method with assistive gain that further improves the tracking performance versus the desired internal air volume and the assistive performance. Meanwhile, our fundamental study is also conducting the isotonic contraction experiments using various IfAs of different sizes (i.e., length, width, number of inflatable chambers, and length per inflatable chamber) to investigate the IfA characteristics of the inner pressure–contraction force, the contraction amount–contraction force, and the inner pressure–contraction amount depending on these variables. Moreover, a fast contraction speed of IfA and a high driving frequency of the InAC control unit might be required to realize the gait support of the wearer's knee flexion and extension motions for elderly people and patients with locomotive syndrome in the maintenance phase. Therefore, it is necessary to adopt not only the optimal size of the IfAs for the assistance of knee joints but also portable compressors with a high drive frequency and with a low burden on the InAC wearer throughout the realistic tests. Additionally, future studies will be required to assess the effectiveness of gait support using the InAC system.

5. Conclusions

In this study, we developed soft inflatable assist clothing called InAC with a lightweight and flexible IfA and proposed a voluntary control method to adjust the compressed air volume supplied from a DC vacuum pump with compressor function to the IfA on the basis of the displacement volume of the BES. The *C–A* and *I–A* profiles included in the BES-based control algorithm were constructed using the results of the IfA isometric contraction experiments. The results of the IfA control verification experiments indicated that the proposed BES-based control method can calculate the desired air volume in accordance with the displacement volume of the BES measured from the subject's lower limb during knee extension movement and then control the IfA air volume to its desired value. Consequently, we have confirmed the usefulness of the developed InAC system through these experiments.

Acknowledgments

This study was partly supported by the Japan Society for the Promotion of Science (JSPS) KAKENHI, Grant-in-Aid for Scientific Research (C), Grant Number 21K12808. We would like to thank Mr. Akihiko Kitano, Mr. Kenichi Hanaoka, and Mr. Sosuke Matsuzawa of the Nagano Prefecture General Industrial Technology Center, Matsumoto, Nagano, Japan, for collaborating on this study.

References

1 United Nations World, Population Prospects 2022: https://www.un.org/development/desa/pd/ (accessed December 2022).
2 H. Terai, Y. Hori, S. Takahashi, K. Tamai, M. Iwamae, M. Hoshino, S. Ohyama, A. Yabu, and H. Nakamura: J. Orthop. Surg. **29** (2021) 3. https://doi.org/10.1177/23094990211060967
3 H. Terai, K. Tamai, S. Takahashi, H. Katsuda, N. Shimada, Y. Hori, Y. Kobayashi, and H. Nakamura: J. Orthop. Sci. **28** (2022) 895. https://doi.org/10.1016/j.jos.2022.05.012
4 A. Nilsson, K. Vreede, V. Häglund, H. Kawamoto, Y. Sankai, and J. Borg: J. Neuroeng. Rehabil. **11** (2014) 92. https://doi.org/10.1186/1743-0003-11-92
5 C. Bach Baunsgaard, U. Vig Nissen, A. Katrin Brust, A. Frotzler, C. Ribeill, Y. B. Kalke, N. León, B. Gómez, K. Samuelsson, W. Antepohl, U. Holmström, N. Marklund, T. Glott, A. Opheim, J. Benito, N. Murillo, J. Nachtegaal, W. Faber, and F. Biering-Sørensen: Spinal Cord **56** (2018) 2. https://doi.org/10.1038/s41393-017-0013-7
6 C. A. McGibbon, A. Sexton, A. Jayaraman, S. Deems-Dluhy, P. Gryfe, A. Novak, T. Dutta, E. Fabara, C. Adans-Dester, and P. Bonato: J. Neuroeng. Rehabil. **15** (2018) 117. https://doi.org/10.1186/s12984-018-0468-6
7 S. H. Lee, H. J. Lee, W. H. Chang, B. O. Choi, J. Lee, J. Kim, G. H. Ryu, and Y. H. Kim: J. Neuroeng. Rehabil. **14** (2017) 123. https://doi.org/10.1186/s12984-017-0333-z
8 E. Martini, S. Crea, A. Parri, L. Bastiani, U. Faraguna, Z. McKinney, R. Molino-Lova, L. Pratali, and N. Vitiello: Sci. Rep. **9** (2019) 7157. https://doi.org/10.1038/s41598-019-43628-2
9 K. Miura, M. Koda, K. Tamaki, M. Ishida, A. Marushima, T. Funayama, H. Takahashi, H. Noguchi, K. Mataki, Y. Yasunaga, H. Kawamoto, Y. Sankai, A. Matsumura, and M. Yamazaki: BMC Musculoskelet. Disord. **22** (2021) 533. https://doi.org/10.1186/s12891-021-04421-3
10 M. Firouzi, E. de Keersmaec, N. Lefeber, S. Roggeman, E. Joos, E. Kerckhofs, D. Beckwée, and E. Swinnen: Top. Geriatr. Rehabil. **39** (2023) 1. https://doi.org/10.1097/tgr.0000000000000384
11 A. Schiele and F. C. T. van der Helm: Appl. Bionics Biomech. **6** (2009) 2. https://doi.org/10.1080/11762320902879961
12 M. Wehner, B. Quinlivan, P. M. Aubin, E. Martinez-Villalpando, M. Baumann, L. Stirling, K. Holt, R. Wood, and C. Walsh: Proc. IEEE Int. Conf. Robotics and Automation (IEEE, 2013) 3362–3369. https://doi.org/10.1109/ICRA.2013.6631046
13 K. Uchiyama, T. Ito, and H. Tomori: J. Robot. Mechatron. **34** (2022) 2. https://doi.org/10.20965/jrm.2022.p0390
14 T. Kadokura, T. Miyazaki, T. Kawase, M. Sogabe, and K. Kawashima: IEEE Access **11** (2023) 35874. https://doi.org/10.1109/ACCESS.2023.3265580
15 C. Thakur, K. Ogawa, and Y. Kurita: J. Robot. Mechatron. **30** (2018) 5. https://doi.org/10.20965/jrm.2018.p0717
16 A. Troncone, T. Amorese, M. Cuciniello, R. Saturno, L. Pugliese, G. Cordasco, C. Vogel, and A. Esposito: Acta Polytech. Hungarica **17** (2020) 2. https://doi.org/10.12700/APH.17.2.2020.2.10
17 Y. Ding, I. Galiana, A. T. Asbeck, S. M. M. De Rossi, J. Bae, T. R. T. Santos, V. L. De Araujo, S. Lee, K. G. Holt, and C. Walsh: IEEE Trans. Neural Syst. Rehabil. Eng. **25** (2017) 2. https://doi.org/10.1109/TNSRE.2016.2523250
18 E. J. Park, T. Akbas, A. Eckert-Erdheim, L. H. Sloot, R. W. Nuckols, D. Orzel, L. Schumm, T. D. Ellis, L.N. Awad, and C. J. Walsh: IEEE Trans. Med. Robot. Bionics **2** (2020) 2. https://doi.org/10.1109/tmrb.2020.2989321
19 H. D. Yang, M. Cooper, A. Eckert-Erdheim, D. Orzel, and C. J. Walsh: IEEE Robot. Autom. Lett. **7** (2022) 3. https://doi.org/10.1109/LRA.2022.3182106
20 L. N. Awad, A. Esquenazi, G. E. Francisco, K. J. Nolan, and A. Jayaraman: J. Neuroeng. Rehabil. **17** (2020) 80. https://doi.org/10.1186/s12984-020-00702-5
21 S. Y. Shin, K. Hohl, M. Giffhorn, L. N. Awad, C.J. Walsh, and A. Jayaraman: J. Neuroeng. Rehabil. **19** (2022) 51. https://doi.org/10.1186/s12984-022-01034-2
22 S. Sridar, P. H. Nguyen, M. Zhu, Q. P. Lam, and P. Polygerinos, Proc. IEEE/RSJ Int. Conf. Intelligent Robots and Systems (IEEE, 2017) 3722–3727. https://doi.org/10.1109/IROS.2017.8206220
23 S. Sridar, Z. Qiao, N. Muthukrishnan, W. Zhang, and P. Polygerinos: Front. Robot. AI **5** (2018) 44. https://doi.org/10.3389/frobt.2018.00044
24 S. Sridar, Z. Qiao, A. Rascon, A. Biemond, A. Beltran, T. Maruyama, C. Kwasnica, P. Polygerinos, and W. Zhang: IEEE Trans. Med. Robot. Bionics **2** (2020) 2. https://doi.org/10.1109/TMRB.2020.2988305
25 T. Yoshioka, S. Kubota, H. Sugaya, N. Arai, K. Hyodo, A. Kanamori, and M. Yamazaki: J. Rural Med. **16** (2021) 1. https://doi.org/10.2185/jrm.2020-024
26 X. Ma, X. Long, Z. Yan, C. Wang, Z. Guo, and X. Wu: Proc. IEEE/ASME Int. Conf. Advanced Intelligent Mechatronics (IEEE, 2019) 589–594. https://doi.org/10.1109/AIM.2019.8868817

27 A. Fleming, N. Stafford, S. Huang, X. Hu, D. P. Ferris, and H. H. Huang: J. Neural Eng. **18** (2021) 4. https://doi.org/10.1088/1741-2552/ac1176
28 A. Tsukahara, T. Miyashita, S. Hirota, N. Shiratori, and H. Nozawa: Japan Patent No. 7212889 (2023). https://www.j-platpat.inpit.go.jp/c1800/PU/JP-2020-195499/90B1B0F54581261956BCE3D061192EC3A2CFB06619832AB7AA16C7EB64396611/11/ja

About the Authors

Atsushi Tsukahara received his M.E. and Ph.D. degrees in engineering from the University of Tsukuba, Japan, in 2007 and 2010, respectively. From 2010 to 2015, he was a postdoctoral fellow of the Center for Cybernics Research, University of Tsukuba, and an associate program manager of the Impulsing Paradigm Change through Disruptive Technologies (ImPACT) Program. From 2015 to 2023, he was an assistant professor at Shinshu University, Japan. Since 2023, he has been an associate professor at the Assistive Robot Center, National Center for Geriatrics and Gerontology, Japan. His research interests are in assistive technology for good health and longevity, human-intention-based physical assistive robot, and artificial intelligence.
(tsukahara@ncgg.go.jp)

Shuta Yamamoto received his B.S. degree from Shinshu University, Japan, in 2023. Since 2023, he has been a graduate student at the Department of Biomedical Engineering, Graduate School of Science and Technology, Shinshu University, Japan. His research interests are in assistive robotics, softmechanics, and biomedical engineering. (23bs228a@shinshu-u.ac.jp)

Sho Hirota received his B.S. and M.E. degrees from Shinshu University, Japan, in 2018 and 2020, respectively. Since 2020, he has been working at VAIO Corporation, Japan. His research interests are in electrical and electronic engineering, mechanism design for computers and computer-related products, and micro-electromechanical systems. (Sho.Hirota@vaio.com)